





Journal of Vibration and Control 2022, Vol. 0(0) 1–16
© The Author(s) 2022
Article reuse guidelines:
sagepub.com/journals-permissions
DOI: 10.1177/10775463221091035
journals.sagepub.com/home/jvc



Passivity-based hierarchical sliding mode control/observer of underactuated mechanical systems

Mohammad-Reza Moghanni-Bavil-Olyaei¹, Jafar Keighobadi¹, Ahmad Ghanbari², and Angelina Olegovna Zekiy³

Abstract

This paper investigates a passivity-based hierarchical SM control (PBHSMC) approach to solve the trajectory tracking issue of a special class of UMSs using unmeasured states and in presence of both unmatched and matched perturbations. First, a passivity-based SM observer (PBSMO) is designed for quick estimation of states in the UMS. Then, we develop a nonlinear two-layer switching surface using feedback passivation. The passivation-based approach ensures global asymptotical convergence of tracking error on the switching surface with the discontinuous term. Moreover, we develop an SMC law that can satisfy reaching mode and sliding mode conditions. Finally, to illustrate the performance of theoretical results, the developed control scheme is assessed by numerical simulation of two case studies including flexible-joint manipulator (FJM) and underactuated surface vessel (USV) systems. The simulation results indicate the superiority of the PBSMO-based PBHSMC scheme over the conventional SMO-based HSMC in suppressing unwanted oscillations of link, low tracking error and overshoot, short settling time, smooth and small control efforts, and also more accurate estimation of state variables with less chattering.

Keywords

passivation, sliding mode observer, hierarchical sliding mode control, underactuated mechanical system, flexible-joint manipulator, underactuated surface vessel

I. Introduction

Under-actuation in mechanical systems may appear due to several reasons, including intrinsic dynamics of the system, deliberate design, and actuator failure. This feature distinguishes a broad category of mechanical systems which are called underactuated mechanical systems (UMSs). In UMSs, some degrees of freedom (DOFs) are not actuated and there is at least one passive DOF. UMSs have many attractive properties such as fewer numbers of actuators, lighter weight, higher safety, tolerance for malfunctioning of actuators, and so forth, while still keeping enough degree of proficiency without reducing the achievable workspace. Some examples of such mechanical systems which have very important applications are flexible systems, marine and aerospace vehicles, mobile and walking robots, etc. (Choukchou-Braham et al., 2013; Liu and Yu, 2013; Spong, 1998).

Design of control strategies and stability analysis of UMSs have been one of the main research subjects in control fields in the last two decades due to their extensive range of applications (Choukchou-Braham et al., 2013; Fantoni et al., 2002; Krafes et al., 2018; Olfati-Saber, 2001). The un-actuated DOFs, strong nonlinearities, and non-holonomic behavior cause the control tasks to be more

complex than those of fully actuated mechanical systems (FAMSs) since they can only be driven by nonlinear dynamic coupling between un-actuated and actuated DOFs. The control problem of UMSs needs to consider global asymptotic stabilization and mismatched uncertainties. Consequently, the control techniques developed for FAMSs usually may not be directly applicable for UMSs (Brockett, 1983). Some control strategies were presented for stabilization and tracking of path objectives of UMSs by assuming complete availability of the state vector and without taking into account the practical issues such as un-modeled dynamics and external disturbances. For example,

¹Faculty of Mechanical Engineering, University of Tabriz, Tabriz, Iran ²School of Engineering Emerging Technologies, University of Tabriz, Tabriz,

³Department of Prosthetic Dentistry, Sechenov First Moscow State Medical University, Moscow, Russia

Received: 2 November 2021; accepted: 3 March 2022

Corresponding author:

Mohammad-Reza Moghanni-Bavil-Olyaei, Faculty of Mechanical Engineering, University of Tabriz, 29 Bahman Blvd., Tabriz 51666, Iran. Email: mr-moghanni@tabrizu.ac.ir

passivity-based control (PBC) methods are developed and proven to be efficient for a special class of UMSs (Ortega et al., 2002; Romero et al., 2018). Also, in (Moghanni-Bavil-Olyaei et al., 2019), a block backstepping-based method was proposed for a special type of UMSs.

From practical point of view, robustness against unmodeled dynamics, parameter variations, and external disturbances is an ever-demanding necessity in designing a control system. SMC as an inherent robust technique shows insensitivity to parametric uncertainty and external noise/ disturbance with known bounds provided that matching condition is satisfied (Utkin et al., 1999; Zhang et al., 2021a). In the last years, SMC-based methods were employed for controlling UMSs (see for example (Ashrafiuon and Erwin, 2008; Xu and Özgüner, 2008; Zhang et al., 2021b)). Wang et al. (Wang et al., 2004) proposed a HSMC algorithm for a special type of 2nd-order UMSs under mismatched and matched disturbance signals. It contains two linear 1st-level switching surfaces separately for the actuated and un-actuated subsystems. By linear combination of the two 1st-level switching surfaces, a 2nd-level switching surface is designable. Overall law of control is synthesized, whereas it includes equivalent control of both subsystems and each subsystem can track the 2nd-level switching surface. With this approach, not only the 2nd-level switching surface has asymptotic stability, but also the 1st-level switching surfaces are asymptotically stable. HSMC design for UMSs with more than two DOFs was further investigated (Qian et al., 2009). However, chattering is practically undesirable in the control input, since highfrequency un-modeled system dynamics may be excited and even damage the plant. Hence, a two-layer linear HSMC scheme was proposed with chattering alleviation as well as robustness against mismatched and matched disturbances for a special type of 2nd-order UMSs (Shi et al., 2017). However, the implementation of conventional HSMC with linear constants 1st-level switching surfaces could be problematic for some reasons. First, approaches that employ linear switching surfaces need huge control inputs to preserve the system trajectory onto the switching surfaces when large state errors exist. Second, by using linear switching surface, nonlinear dynamics is replaced with linear one. So, the global dynamics of the UMS may not be fitted (Tokat et al., 2015). The design of the switching surface is of most importance because it highly affects the performance of the system. In this regard, SMC approaches including a nonlinear switching surface and a time-varying switching surface have been presented for UMSs (Kurode et al., 2012; Singh and Ha, 2019; Xu et al., 2013). An integral SMC was designed for a wheeled underactuated mobile robot subject to both unmatched and matched uncertainties (Xu et al., 2013). A nonlinear switching surface was presented to design SMC for a slosh-free motion in a simple pendulum to improve its damping as a class of second-order **UMS** with unmatched uncertainties (Kurode et al., 2012). Recently, an SMC together with the fastterminal method was assessed by linear combination of two

hierarchical switching surfaces for a special type of 2-DOF UMSs in presence of bounded uncertainties and disturbances (Singh and Ha, 2019). In this paper, a nonlinear hierarchical switching surface is developed which can efficiently improve the closed-loop performance.

As mentioned before, in most of the previous works on control of UMS, there is a common assumption for complete availability of the state vector. In practice, the implementation of a control system relies on the availability of state variables to produce a feedback control signal. Encoders can precisely measure all the displacements, but the computed measurements of velocity states from the encoder, which are indirectly available for controller design, are commonly perturbed by stochastic noises. Hence, a robust state estimation method is required for accurate estimation of velocity signals against both exogenous disturbance and model uncertainty. Among state estimation methods presented in the literature (Almeida et al., 2015; Chalhoub et al., 2006; Chang et al., 2021; Chang and Jin, 2022; Chawengkrittayanont and Pukdeboon, 2019; Liu et al., 2020; Xu and Rahman, 2012), sliding mode observer (SMO) is an attractive choice for UMSs, owing to rapid dynamics and powerful robustness against measurement noise, disturbance, and parameter deviations. In addition, SMO has other advantages over extended Kalman filter (EKF) including simpler algorithm, less restrictive design, no requirement for extensive computations (e.g., noise statistics), and changeable dynamical performance (Xu and Rahman, 2012). Nevertheless, chattering created by discontinuous switching function is an unavoidable issue in SMO (Almeida et al., 2015; Chalhoub et al., 2006; Chawengkrittayanont and Pukdeboon, 2019). Hence, the key to success in state estimation by SMO is to lower the chattering and improve the accuracy of low-speed estimation. An SMO should estimate the components of state vector in a special type of UMSs using hyperbolic tangent function instead of the conventional switching function to significantly reduce the chattering (Liu et al., 2020).

Passivity provides powerful framework based on energy concepts for stability analysis of systems, especially for nonlinear systems (Arimoto, 1996). For a passive system, the flowing of energy is always greater than the energy that flows out (Brogliato et al., 2020). The basic idea of passivity theory is that the passive properties of a system can ensure internal stability of the system by using input-output characteristics. In addition, the passivation problem that is sometimes called passification, is understood as finding an appropriate controller to make the closed-loop system passive (Fradkov, 2003; Jahangiri et al., 2018; Seron et al., 1994). Some interesting results with passivity and passivation of SMC for different types of systems have been presented in the literature. For instance, in (Kikuuwe et al., 2010), a proxy-based SMC was presented using passivity theory for position control of robotic systems. A passivity-based robust continuous SMC was also developed in (Wei and Mottershead, 2017) for underactuated nonlinear wing sections in presence of both unmatched and matched uncertainties. Nevertheless, the design method is Moghanni-Bavil-Olyaei et al.

unsystematic and rather complicated for extension. Recently, a passivity-based SMC/observer was examined for stabilization purpose of a second-order nonlinear system affected by matched disturbances (Chang, 2019). However, the investigated approaches are not directly implementable for tracking problem of UMSs.

In this paper, motivated by the above discussed background, our main contribution is as follows. We develop a robust passivity-based hierarchical SMC (PBHSMC) for path tracking of a special class of UMSs under matched perturbations and the unmatched type as well. First, through the designed passivity-based SMO (PBSMO) for UMSs, the global asymptotic observation of the state variables is obtainable even under disturbance and parameter vagueness. The proposed observer is designed by passivation of observation error dynamics. Next, passivity theory and energy-shaping strategies are utilized to develop a hierarchical nonlinear switching surface where global asymptotical stability is guaranteed. The proposed passivation-based control law has a discontinuous control action with a nonlinear equivalent control part and ensures asymptotic convergence of the system to the switching surface. For the special class of UMS subjected to unmatched disturbances and uncertainties, it is shown that the proposed method has the capability of asymptotical stabilization of the closed-loop system. An SMC law is further developed such that the reaching and sliding conditions are satisfied.

In rest of the paper, Section 2 briefly introduces the UMSs modeling and control objectives. Section 3 represents PBSMO for UMSs following the design of a conventional SMO for UMSs. Next, development of our proposed observer for state estimation is explained. Section 4 presents the PBHSMC for the considered class of UMSs. The conventional HSMC approach is explained first and then the design method of the control system is elaborated in detail. In Section 5, PBSMO-based PBHSMC for trajectory tracking of SFJM and USV are represented. Following simulation results analysis, conclusions are released in Section 6.

2. System model

State-space equations of a special class of UMSs affected by uncertainties/disturbances are represented as

$$\dot{x}_1(t) = x_2(t)
\dot{x}_2(t) = f_1(x,t) + g(x,t)u + d_1(x,t)
\dot{x}_3(t) = x_4(t)
\dot{x}_4(t) = f_2(x,t) + d_2(x,t)$$
(1)

Assumption 1.

$$g(x,t) \neq 0 \tag{2}$$

In equation (1), x_1,x_2,x_3,x_4 stand for state variables and $f_1(.,.), f_2(.,.)$, and g(.,.) represent bounded nonlinear terms. Unknown unmatched uncertainties and disturbances are denoted by terms d_1 and d_2 . Now, the control objective is considered as design of a passivity-based SMC/SMO for trajectory tracking problem such that the drawbacks of conventional SMC are improved in terms of reaching time and system performance.

3. Passivity-based SMO

For UMS of equation (1), we assume x_1 and x_3 to be directly measurable state variables, and their corresponding velocities x_2 and x_4 are unmeasurable. Here, a robust observer based on passivity and SMC techniques is designed to estimate the unmeasured states under effect of model uncertainty/disturbances. Following explaining conventional SMO, we release PBSMO to address the state estimation problem by compelling the error dynamics of observation to match a stored energy function, in such a way that the passivity properties are preserved.

3.1 Conventional SMO

For system (1), the following measurable output y is chosen as

$$\begin{bmatrix} \dot{x}_1 \\ \dot{x}_2 \\ \dot{x}_3 \\ \dot{x}_4 \end{bmatrix} = \begin{bmatrix} x_2 \\ f_1 \\ x_4 \\ f_2 \end{bmatrix} + \begin{bmatrix} 0 \\ g \\ 0 \\ 0 \end{bmatrix} u + \begin{bmatrix} 0 \\ d_1 \\ 0 \\ d_2 \end{bmatrix}$$

$$y = \begin{bmatrix} x_1 & x_3 \end{bmatrix}^T$$
(3)

The state equations of conventional SMO for this class of UMSs are designable as

$$\begin{bmatrix} \dot{\widehat{x}}_{1} \\ \dot{\widehat{x}}_{2} \\ \dot{\widehat{x}}_{3} \\ \dot{\widehat{x}}_{4} \end{bmatrix} = \begin{bmatrix} \widehat{x}_{2} \\ \widehat{f}_{1} + \widehat{g}u \\ \widehat{x}_{4} \\ \widehat{f}_{2} \end{bmatrix} + \begin{bmatrix} \eta_{1}\widetilde{x}_{1} + \mu_{1}\operatorname{sgn}(\widetilde{x}_{1}) \\ \eta_{2}\widetilde{x}_{1} + \mu_{2}\operatorname{sgn}(\widetilde{x}_{1}) \\ \eta_{3}\widetilde{x}_{3} + \mu_{3}\operatorname{sgn}(\widetilde{x}_{3}) \\ \eta_{4}\widetilde{x}_{3} + \mu_{4}\operatorname{sgn}(\widetilde{x}_{3}) \end{bmatrix}$$
(4)

with μ_i and η_i being Luenberger observer and sliding term positive gains. \widehat{f}_1 , \widehat{f}_2 , \widehat{g} represent updated f_1 , f_2 , g with estimated values for state vector. Thus, the error dynamics of the observer is expressed by

$$\begin{bmatrix} \dot{\tilde{x}}_{1} \\ \dot{\tilde{x}}_{2} \\ \dot{\tilde{x}}_{3} \\ \dot{\tilde{x}}_{4} \end{bmatrix} = \begin{bmatrix} \tilde{x}_{2} \\ \hat{f}_{1} \\ \tilde{x}_{4} \\ \tilde{f}_{2} \end{bmatrix} - \begin{bmatrix} \eta_{1}\tilde{x}_{1} + \mu_{1}\operatorname{sgn}(\tilde{x}_{1}) \\ \eta_{2}\tilde{x}_{1} + \mu_{2}\operatorname{sgn}(\tilde{x}_{1}) \\ \eta_{3}\tilde{x}_{3} + \mu_{3}\operatorname{sgn}(\tilde{x}_{3}) \\ \eta_{4}\tilde{x}_{3} + \mu_{4}\operatorname{sgn}(\tilde{x}_{3}) \end{bmatrix} + \begin{bmatrix} 0 \\ d_{1} \\ 0 \\ d_{2} \end{bmatrix}$$
(5)

in which, $\tilde{x}_i = x_i - \hat{x}_i$ stand for estimation error, and $\tilde{f}_1 = f_1 - \hat{f}_1$, and $\tilde{f}_2 = f_2 - \hat{f}_2$ are uncertainty terms. Also, we assumed that $g = \hat{g}$.

Thereby, the observation error vector is obtained as

$$\dot{\tilde{x}} = \tilde{f} - \eta [\tilde{x}_1 or \ \tilde{x}_3] + \mu \operatorname{sgn}(\tilde{x}_1 or \ \tilde{x}_3)$$
 (6)

where
$$\tilde{f} = \begin{bmatrix} \tilde{x}_2 & \tilde{f}_1 + d_1 & \tilde{x}_4 & \tilde{f}_2 + d_2 \end{bmatrix}^T$$
, $\eta = \begin{bmatrix} \eta_1 & \eta_2 \\ \eta_3 & \eta_4 \end{bmatrix}^T$, and $\begin{bmatrix} \mu_1 & \mu_2 & \mu_3 & \mu_4 \end{bmatrix}^T$.

The output of equation (5) can be considered as

$$s_{ob} = C\tilde{x} C = \begin{bmatrix} 1 & 0 & 0 & 0 \\ 0 & 0 & 1 & 0 \end{bmatrix}$$
 (7)

Hence, when the system slides on the switching surfaces, its sliding dynamics is expressed by

$$\dot{s}_{ob} = C \left(\tilde{f} - \eta \left[\tilde{x}_1 or \ \tilde{x}_3 \right] + \mu \operatorname{sgn} \left(\tilde{x}_1 or \ \tilde{x}_3 \right) \right) = 0 \quad (8)$$

3.2 Passivity-based sliding mode observer

Now, we consider the observer (4) to take the following form

$$\begin{bmatrix} \hat{x}_1 \\ \hat{x}_2 \\ \hat{x}_3 \\ \hat{x}_4 \end{bmatrix} = \begin{bmatrix} \hat{x}_2 \\ \hat{f}_1 + \hat{g}u \\ \hat{x}_4 \\ \hat{f}_2 \end{bmatrix} + \begin{bmatrix} \eta_1 \tilde{x}_1 - \mu_1 v_1 \\ \eta_2 \tilde{x}_1 - \mu_2 v_1 \\ \eta_3 \tilde{x}_3 - \mu_3 v_2 \\ \eta_4 \tilde{x}_3 - \mu_4 v_2 \end{bmatrix}$$
(9)

in which, $sgn(\tilde{x}_1)$ and $sgn(\tilde{x}_3)$ are respectively included in new terms v_1 and v_2 . The error dynamics of the observer is expressed by

$$\begin{bmatrix} \dot{\tilde{x}}_1 \\ \dot{\tilde{x}}_2 \\ \dot{\tilde{x}}_3 \\ \dot{\tilde{x}}_4 \end{bmatrix} = \begin{bmatrix} \tilde{x}_2 \\ \tilde{f}_1 \\ \tilde{x}_4 \\ \tilde{f}_2 \end{bmatrix} + \begin{bmatrix} -\eta_1 \tilde{x}_1 + \mu_1 v_1 \\ -\eta_2 \tilde{x}_1 + \mu_2 v_1 \\ -\eta_3 \tilde{x}_3 + \mu_3 v_2 \\ -\eta_4 \tilde{x}_3 + \mu_4 v_2 \end{bmatrix} + \begin{bmatrix} 0 \\ d_1 \\ 0 \\ d_2 \end{bmatrix}$$
(10)

From equation (10), we can write the dynamics of \tilde{x} in matrix form as

$$\dot{\tilde{x}}(t) = A\tilde{x}(t) + B_1 v(t) + B_2 \overline{f}(t)$$

$$\tilde{y}(t) = C\tilde{x}(t)$$
(11)

with

$$A = \begin{bmatrix} -\eta_1 & 1 & 0 & 0 \\ -\eta_2 & 0 & 0 & 0 \\ 0 & 0 & -\eta_3 & 1 \\ 0 & 0 & -\eta_4 & 0 \end{bmatrix}, B_1 = \begin{bmatrix} \mu_1 & 0 \\ \mu_2 & 0 \\ 0 & \mu_3 \\ 0 & \mu_4 \end{bmatrix},$$
$$v(t) = \begin{bmatrix} v_1(t) \\ v_2(t) \end{bmatrix}, B_2 = \begin{bmatrix} 0 & 0 \\ 1 & 0 \\ 0 & 0 \\ 0 & 1 \end{bmatrix}$$

$$\overline{f}(t) = \begin{bmatrix} \overline{f}_1(t) \\ \overline{f}_2(t) \end{bmatrix} = \begin{bmatrix} \tilde{f}_1(t) + d_1(t) \\ \tilde{f}_2(t) + d_2(t) \end{bmatrix}, C = \begin{bmatrix} 1 & 0 & 0 & 0 \\ 0 & 0 & 1 & 0 \end{bmatrix}$$

Taking Laplace transformation of both sides of equation (11) results in

$$\tilde{X}_1(s) = \frac{1}{s^2 + \eta_1 s + \eta_2} \overline{F}_1(s) + \frac{\mu_1 s + \mu_2}{s^2 + \eta_1 s + \eta_2} V_1(s) \quad (12)$$

$$\tilde{X}_3(s) = \frac{1}{s^2 + \eta_3 s + \eta_4} \overline{F}_2(s) + \frac{\mu_3 s + \mu_4}{s^2 + \eta_3 s + \eta_4} V_2(s) \quad (13)$$

 $\dot{s}_{ob} = C \bigg(\tilde{f} - \eta \bigg[\tilde{x}_1 or \ \tilde{x}_3 \bigg] + \mu \mathrm{sgn} \bigg(\tilde{x}_1 or \ \tilde{x}_3 \bigg) \bigg) = 0 \quad (8) \quad \frac{\tilde{X}_1(s) = L(\tilde{x}_1(t)), \quad \tilde{X}_3(s) = L(\tilde{x}_3(t)), \quad \overline{F}_1(s) = L(\overline{f}_1(t)), \quad \overline{F}_2(s) = L(\overline{f}_2(t)), \quad V_1(s) = L(v_1(t)), \quad \text{and} \quad V_2(s) = L(\overline{f}_1(t)) \bigg)$ $=L(v_2(t))$. We define functions w_1 and w_2 as

$$W_1(s) = \frac{\overline{F}_1(s)}{(\mu_1 s + \mu_2)}$$
 then $\dot{w}_1 + \left(\frac{\mu_2}{\mu_1}\right) w_1 = \frac{1}{\mu_1} \overline{f}_1$ (14)

$$W_2(s) = \frac{\overline{F}_2(s)}{(\mu_3 s + \mu_4)}$$
 then $\dot{w}_2 + \left(\frac{\mu_4}{\mu_3}\right) w_2 = \frac{1}{\mu_3} \overline{f}_2$ (15)

where $W_1(s) = (w_1(t))$ and $W_2(s) = L(w_2(t))$. Since $\tilde{f}_1(t)$, $f_2(t)$ $d_1(t)$, and $d_2(t)$ are uniformly bounded, we have $|w_1(t)| < \overline{w}_1$ and $|w_2(t)| < \overline{w}_2$, where \overline{w}_1 and \overline{w}_2 are known positive constants. Now, we can rewrite equations (12) and (13) as

$$\tilde{X}_{1}(s) = \frac{\mu_{1}s + \mu_{2}}{s^{2} + \eta_{1}s + \eta_{2}} \frac{F_{1}(s)}{\mu_{1}s + \mu_{2}} + \frac{\mu_{1}s + \mu_{2}}{s^{2} + \eta_{1}s + \eta_{2}}$$

$$V_{1}(s) = \frac{\mu_{1}s + \mu_{2}}{s^{2} + \eta_{1}s + \eta_{2}} (W_{1}(s) + V_{1}(s))$$

$$= H_{1}(s)(W_{1}(s) + V_{1}(s))$$
(16)

$$\begin{split} \tilde{X}_{3}(s) &= \frac{\mu_{3}s + \mu_{4}}{s^{2} + \eta_{3}s + \eta_{4}} \frac{\overline{F}_{2}(s)}{\mu_{3}s + \mu_{4}} + \frac{\mu_{3}s + \mu_{4}}{s^{2} + \eta_{3}s + \eta_{4}} V_{2}(s) \\ &= \frac{\mu_{3}s + \mu_{4}}{s^{2} + \eta_{3}s + \eta_{4}} (W_{2}(s) + V_{2}(s)) \\ &= H_{2}(s)(W_{2}(s) + V_{2}(s)) \end{split} = 2 \begin{bmatrix} \frac{\mu_{2}\eta_{2} + (\mu_{1}\eta_{1} - \mu_{2})\omega^{2}}{(\eta_{2} - \omega^{2})^{2} + (\eta_{1}\omega)^{2}} & 0 \\ 0 & \frac{\mu_{4}\eta_{4} + (\mu_{3}\eta_{3} - \mu_{4})\omega^{2}}{(\eta_{4} - \omega^{2})^{2} + (\eta_{3}\omega)^{2}} \end{bmatrix}$$

In which, $H_1(s)$ and $H_2(s)$ stand for transfer functions.

Lemma 1. (Khalil, 2002).

Regarding $H(s) = C(sI - A)^{-1}B$ a proper transfer matrix with Hurwitz A, observable (C,A), and controllable (A,B); then, H(s) is strictly positive-real (SPR) if there exists a symmetric positive definite matrix $P = P^T > 0$, L, and a scalar constant $\varepsilon > 0$ such that

$$PA + A^{T}P = -L^{T}L - \varepsilon P$$

$$PB = C^{T}$$
(18)

Lemma 2. (Tao and Ioannou, 1988).

A real rational and strictly proper transfer matrix H(s) of the complex variable s is SPR if

- (i) H(s) is real for all real s and all elements of H(s) are analytic in Re $\{s\} > 0$, that is, H(s) is Hurwitz (H(s))has no pole in $Re\{s\} > 0$,
- (ii) $H(j\omega) + H^T(-j\omega) > 0 \forall \omega \in (-\infty,\infty),$
- (iii) $\lim_{\omega \to \infty} \omega^2 \{ H(j\omega) + H^T(-j\omega) \} > 0$

Lemma 3. The transfer matrix

$$H(s) = \begin{bmatrix} H_1(s) & 0\\ 0 & H_2(s) \end{bmatrix}$$

$$= \begin{bmatrix} \frac{\mu_1 s + \mu_2}{s^2 + \eta_1 s + \eta_2} & 0\\ 0 & \frac{\mu_3 s + \mu_4}{s^2 + \eta_3 s + \eta_4} \end{bmatrix}$$
(19)

is SPR if $0 < \mu_2 < \mu_1 \eta_1$ and $0 < \mu_4 < \mu_3 \eta_3$. Proof:

We have

$$=\begin{bmatrix} H(j\omega) + H^{T}(-j\omega) \\ \frac{\mu_{2} + j\mu_{1}\omega}{\eta_{2} - \omega^{2} + j\eta_{1}\omega} + \frac{\mu_{2} - j\mu_{1}\omega}{\eta_{2} - \omega^{2} - j\eta_{1}\omega} & 0 \\ 0 & \frac{\mu_{4} + j\mu_{3}\omega}{\eta_{4} - \omega^{2} + j\eta_{3}\omega} + \frac{\mu_{4} - j\mu_{3}\omega}{\eta_{4} - \omega^{2} - j\eta_{3}\omega} \end{bmatrix}$$

$$=2\begin{bmatrix} \frac{\mu_{2}(\eta_{2}-\omega^{2})+\mu_{1}\eta_{1}\omega^{2}}{\left(\eta_{2}-\omega^{2}\right)^{2}+\left(\eta_{1}\omega\right)^{2}} & 0\\ 0 & \frac{\mu_{4}(\eta_{4}-\omega^{2})+\mu_{3}\eta_{3}\omega^{2}}{\left(\eta_{4}-\omega^{2}\right)^{2}+\left(\eta_{3}\omega\right)^{2}} \end{bmatrix}$$

$$=2\begin{bmatrix} \frac{\mu_{2}\eta_{2}+(\mu_{1}\eta_{1}-\mu_{2})\omega^{2}}{(\eta_{2}-\omega^{2})^{2}+(\eta_{1}\omega)^{2}} & 0\\ 0 & \frac{\mu_{4}\eta_{4}+(\mu_{3}\eta_{3}-\mu_{4})\omega^{2}}{(\eta_{4}-\omega^{2})^{2}+(\eta_{2}\omega)^{2}} \end{bmatrix}$$

Based on the above equation and concept of SPR, the transfer matrix H(s) is SPR if the conditions $(\mu_1 \eta_1 - \mu_2) > 0$ and $(\mu_3 \eta_3 - \mu_4) > 0$ hold.

Lemma 4. (See Ref. (Khalil, 2002)).

Assuming a nonlinear dynamics system as

$$\dot{x} = f(x) + g(x)u$$

$$y = h(x)$$
(20)

Providing strict passivity of equation (20), the origin equilibrium point of $\dot{x}(t) = f(x)$ with u = 0 is asymptotically stable. In addition, a radially unbounded storage function should result in global asymptotic stability.

Definition 1. (Passivity theory (Khalil, 2002)).

The nonlinear system equation (20) is called passive if for a non-negative-valued function V(t)

$$V(x(t)) - V(x(0)) \le \int_0^t u^T(\tau)y(\tau)d\tau - \int_0^t N(x(\tau))d\tau$$
(21)

where N(x) is a positive semi-definite (PSD) function or zero. If N(x) is positive definite (PD), then the nonlinear system is called strictly passive.

Theory 1. For the UMS (1), the PBSMO is proposed as

$$\begin{bmatrix} \hat{\vec{x}}_1 \\ \hat{\vec{x}}_2 \\ \hat{\vec{x}}_3 \\ \hat{\vec{x}}_4 \end{bmatrix} = \begin{bmatrix} \hat{x}_2 \\ \hat{f}_1 + \hat{g}u \\ \hat{x}_4 \\ \hat{f}_2 \end{bmatrix} + \begin{bmatrix} \eta_1 \tilde{x}_1 - \mu_1 v_1 \\ \eta_2 \tilde{x}_1 - \mu_2 v_1 \\ \eta_3 \tilde{x}_3 - \mu_3 v_2 \\ \eta_4 \tilde{x}_3 - \mu_4 v_2 \end{bmatrix}$$
(22)

in which the discontinuous sgn term is reachable as

$$v_1 = -\left(\overline{w}_1 + \gamma_1\right) \operatorname{sgn}\left(\tilde{x}_1\right) + r_1 \tag{23}$$

$$v_2 = -\left(\overline{w}_2 + \gamma_2\right) \operatorname{sgn}\left(\tilde{x}_3\right) + r_2 \tag{24}$$

where $r_1(t)$ and $r_2(t)$ are fictitious inputs and $\gamma_1, \gamma_2 > 0$ are design parameters. If the gains η_i , μ_i can be selected to obtain SPR H(s), observation efficiency tends to satisfy $\lim \widehat{\mathbf{x}}(t) \to \mathbf{x}(t)$.

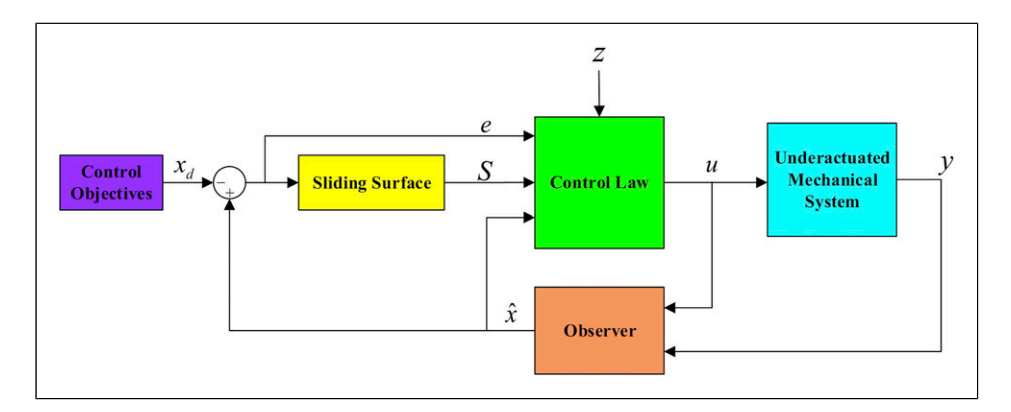


Figure 1. Proposed Passivity-based hierarchical sliding mode control architecture.

Proof.

In accordance with equations (16), (17), (23), and (24), we may express error dynamics \tilde{x} as

$$\dot{\tilde{x}} = A\tilde{x} - B_1 \left(\overline{w} + \gamma\right) \operatorname{sgn}\left(\tilde{x}_{1,3}\right) + B_1(r+w)$$

$$\tilde{y} = C\tilde{x}$$
(25)

where

$$(\overline{w} + \gamma) \operatorname{sgn}(\tilde{x}_{1,3}) = \begin{bmatrix} (\overline{w}_1 + \gamma_1) \operatorname{sgn}(\tilde{x}_1) \\ (\overline{w}_2 + \gamma_2) \operatorname{sgn}(\tilde{x}_3) \end{bmatrix}$$

$$r = \begin{bmatrix} r_1 \\ r_2 \end{bmatrix}, w = \begin{bmatrix} w_1 \\ w_2 \end{bmatrix}$$

In above system, r and y can be taken as the new inputs and the outputs for the system, respectively. According to Lemma 3, we can select the parameters η_i and μ_i to impose the inequality constraints $0 < \mu_2 < \mu_1 \eta_1$ and $0 < \mu_4 < \mu_3 \eta_3$, so that the transfer matrix H(s) is SPR. Based on Lemma 1, there exist matrices $P \in \mathbb{R}^{4 \times 4}$ and $L \in \mathbb{R}^{4 \times 4}$ such that

$$PA + A^{T}P = -L^{T}L - \varepsilon P$$

$$PB_{1} = C^{T}$$

Using Definition 1 and the storage function as $V = \tilde{x}^T P \tilde{x}$ leads to

$$\begin{split} r^T \tilde{y} - \dot{V} &= r^T \tilde{y} - \frac{\partial V}{\partial \tilde{x}} \left(A \tilde{x} - B_1 \left(\overline{w} + \gamma \right) \operatorname{sgn} \left(\tilde{x}_{1,3} \right) + B_1 (r + w) \right) \\ &= r^T C \tilde{x} - \tilde{x}^T P \left(A \tilde{x} - B_1 \left(\overline{w} + \gamma \right) \operatorname{sgn} \left(\tilde{x}_{1,3} \right) + B_1 (r + w) \right) \\ &= r^T C \tilde{x} - \frac{1}{2} \tilde{x}^T \left(P A + A^T P \right) \tilde{x} + \left(\overline{w} + \gamma \right) \left| \tilde{x}_{1,3} \right| - \tilde{x}^T P B_1 (r + w) \\ &\geq \frac{1}{2} \tilde{x}^T \left(L^T L + \varepsilon P \right) \tilde{x} + \gamma \left| \tilde{x}_{1,3} \right| \geq \frac{1}{2} \varepsilon V + \gamma \left| \tilde{x}_{1,3} \right| \end{split}$$

time integrating of both sides over $\tau \in [0,t]$ gives

$$\int_0^t r^T(\tau)\tilde{y}(\tau)d\tau - \int_0^t N(\tau)d\tau \ge V(t) - V(0)$$

in which $N = \frac{1}{2} \varepsilon V + \gamma |\tilde{x}_{1,3}| > 0$. Based on Definition 1, the system of equation (25) is strictly passive where r and y denote the new input and output, respectively. We can conclude from Lemma 4, $\lim_{t \to \infty} \widehat{x}(t) = x(t)$ and $\lim_{t \to \infty} \widehat{x}(t) = 0$.

4. Design of PBHSMC

The energy-based passivity technique is applied for stability analysis of the nonlinear system and feedback control design. In this section, design of the passivity-based hierarchical SMC law is presented in detail for the class of UMSs to realize control objective. First, conventional hierarchical sliding mode controller is described. Then, we devise passivity-based hierarchical SMC to push the states trajectory toward the origin along the switching surface while the passivity conditions of the system are preserved.

First of all, it is essential to remember some related results and definitions of passivity concept and PBC.

Definition 2. (See Refs. (Choukchou-Braham et al., 2013) and (Khalil, 2002)).

The nonlinear system equation (20) is called passive if a non-negative-valued stored energy function V(t) exists which satisfies the following energy balancing equation

$$\underbrace{V(x(t)) - V(x(0))}_{\text{stored}} \leq \underbrace{\int_{0}^{t} u^{T}(\tau) y(\tau) d\tau}_{\text{supplied}} - \underbrace{\int_{0}^{t} N(x(\tau)) d\tau}_{\text{dissipated}}$$
(26)

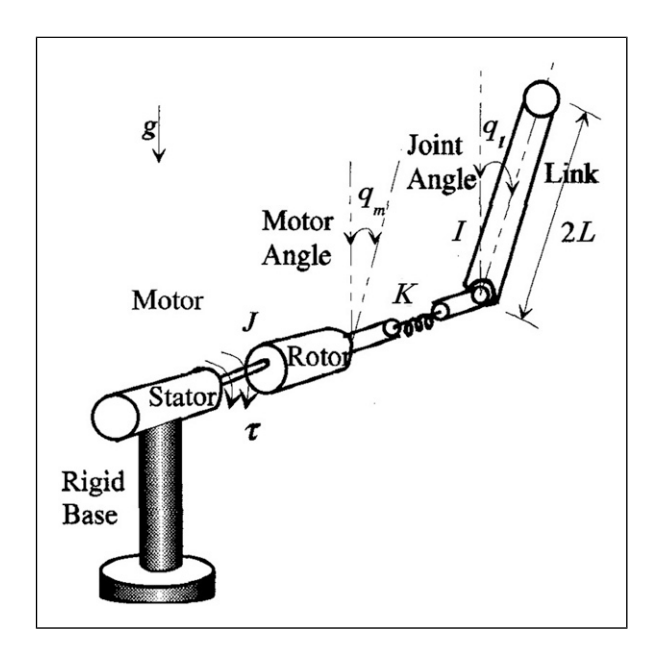


Figure 2. A schematic of flexible single-link and joint manipulator.

where N(x) is a PSD term. A PD N(x) implies strict passivity of the nonlinear system.

For dynamics system equation (20), by f(0) = 0, h(0) = 0, and with proper and PD V(x), global asymptotic stability of the equilibrium point, x = 0 can be easily concluded (Chang, 2019). Furthermore, the system equation (20) is called feedback passive provided that the following feedback control law be exists

$$u = \Phi(x, v) \tag{27}$$

under the condition that the system will be passive with new input $v \in \mathbb{R}$.

Definition 3. Let the system equation (20) be given with h(0) = 0 and f(0) = 0. This nonlinear system is zero-state observable if $y = h(x) \equiv 0$ follows that $\lim_{t \to \infty} x(t) = 0$ (Khalil, 2002).

Lemma 5. Let the nonlinear system equation (20) be given with h(0) = 0 and f(0) = 0. If the two below properties are satisfied (Khalil, 2002):

- a) passive with a non-negative-valued stored energy function.
- b) detectable of zero-state,

then x=0 becomes stabilizable using $u=-\varphi(y)$ with $y\varphi(y)>0$ and $\varphi(0)=0$ for all $y\neq 0$, globally. Therefore, starting by every initial condition, $\lim_{t\to\infty} x(t)=0$. Furthermore, if the system is SPR, then the origin will have global asymptotic stability even if u=0.

Table 1. Values of the single-link flexible joint manipulator parameters.

Symbol	Definition	Value	Unit
2L	Length of link	2	m
1	Inertia of link	2	kg.m ²
m	Mass of link	2	kg
Κ	Joint stiffness	10	N.m/rad
B_m	Motor damping	0.5	N.s/rad
J	Inertia of motor	0.5	kg.m ²
g	Gravitational constant	9.81	m/s ²

4.1. Conventional HSMC

In underactuated systems, conventional hierarchical SMC leads to a two-layer proportional-derivative switching surface which is two constant linear switching surfaces (Wang et al., 2004) and in which the magnitude of the constants determines performance of the system.

Consider an underactuated nonlinear system as

$$\dot{x}_1 = x_2
\dot{x}_2 = f_1 + g_1 u
\dot{x}_3 = x_4
\dot{x}_4 = f_2 + g_2 u$$
(28)

To design conventional HSMC, tracking errors e_i are defined as

$$e_i = x_i - x_{id} \tag{29}$$

where x_{id} stand for desired states value. Then, two first-layer proportional-derivative switching surfaces are constructible as

$$s_1 = e_2 + c_1 e_1 \tag{30}$$

$$s_2 = e_4 + c_2 e_3 \tag{31}$$

where the positive fixed gains c_1 and c_2 will assign convergence rate of tracking errors to switching surfaces. Finally, the second-layer switching surface for the system with relative degree 2 is definable as

$$S = \alpha s_1 + \beta s_2 \tag{32}$$

in which α and β are positive control gains.

Considering $\dot{s}_1 = 0$ and $\dot{s}_2 = 0$ and applying f_1, f_2, \hat{g}_1 , and \hat{g}_2 as updated versions of f_1, f_2, g_1 , and g_2 by observer states, the equivalent control law is obtainable as

$$u_{eq1} = -\frac{1}{\hat{g}_1} \left(\hat{f}_1 + c_1 \dot{e}_1 - \dot{x}_{2d} \right)$$
 (33)

$$u_{eq2} = -\frac{1}{\hat{g}_2} \left(\hat{f}_2 + c_2 \dot{e}_3 - \dot{x}_{4d} \right) \tag{34}$$

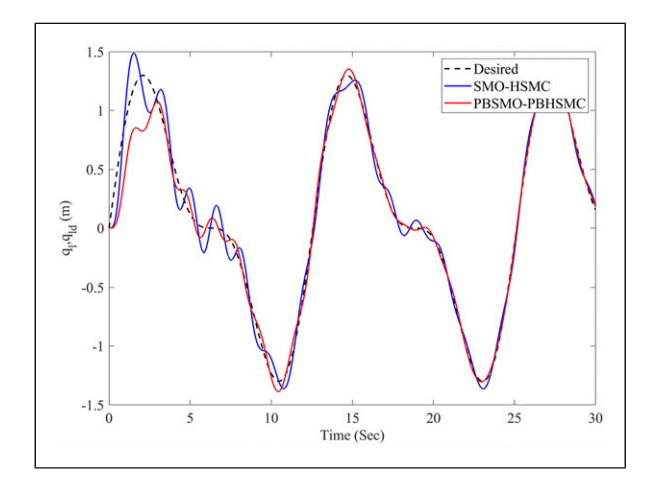


Figure 3. Angular displacement q_l through sliding mode observer-based hierarchical sliding mode control and proposed passivity-based sliding mode observer-based passivity-based hierarchical sliding mode control.

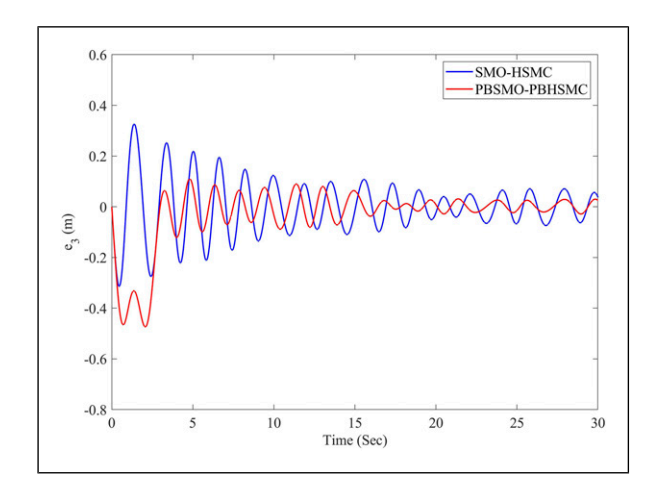


Figure 4. Tracking error e₃ through sliding mode observer-based hierarchical sliding mode control and proposed passivity-based sliding mode observer-based passivity-based hierarchical sliding mode control.

Finally, for the UMS equation (28) and the switching surface equation (32), the following controller was employed in most studies to satisfy reaching mode and sliding mode conditions (Chen et al., 2020; Shi et al., 2017; Wang et al., 2004; Zehar et al., 2018)

$$u = u_{eq1} + u_{eq2} + u_{sw} (35)$$

in which u_{sw} is the switching control as

$$u_{sw} = \frac{-1}{\alpha \widehat{g}_1 + \beta \widehat{g}_2} (k_1 \operatorname{sgn}(S) + k_2 S)$$
 (36)

where $k_1 > 0$ is switching gain, and $k_2 > 0$ is reaching control gain. These tuneable gains specify convergence rate of trajectories to the switching surface. For large initial off-tracks from desired trajectory, according to equation

(35), large compensator actions lead to extreme oscillations of control signals and actuator saturation, accordingly (Hippe, 2006). In order to address these drawbacks, an observer-based and passivity-based hierarchical SMC is proposed in the following.

4.2. Passivity-based hierarchical sliding mode controller

For observer-based and passivity-based HSMC design, the error of states is introduced as

$$e_i = x_i - x_{id} = \hat{x}_i - x_{id} + \tilde{x}_i, \quad i = 1, 2, 3, 4$$
 (37)

Taking time derivatives guide to

$$\dot{e}_{1} = \hat{x}_{2} - x_{2d} + \tilde{x}_{2} = \dot{x}_{1} - \dot{x}_{1d}
\dot{e}_{2} = \hat{f}_{1} + \hat{g}u + d_{1} - \dot{x}_{2d} + \tilde{f}_{1} + \tilde{g}u = \dot{x}_{2} - \dot{x}_{2d}
\dot{e}_{3} = \hat{x}_{4} - x_{4d} + \tilde{x}_{4} = \dot{x}_{3} - \dot{x}_{3d}
\dot{e}_{4} = \hat{f}_{2} + d_{2} - \dot{x}_{4d} + \tilde{f}_{2} = \dot{x}_{4} - \dot{x}_{4d}$$
(38)

Supposing $\Sigma_1(e_1,\lambda_1,c_1)$ and $\Sigma_2(e_3,\lambda_2,c_2)$ as two scalar potential functions with positive design gains $c_1,c_2\in\mathbb{R}$ and $\lambda_1,\lambda_2\in\mathbb{R}$, and the first derivatives of Σ_1 and Σ_2 as $\sigma_1(e_1,\lambda_1,c_1)=\frac{d\Sigma_1(e_1,\lambda_1,c_1)}{de_1}$ and $\sigma_2(e_3,\lambda_2,c_2)=\frac{d\Sigma_2(e_3,\lambda_2,c_2)}{de_3}$, all should have the following three properties (Arimoto, 1996):

- (P1) $\Sigma_1(e_1,\lambda_1,c_1) > 0$ for $e_1 \neq 0$, and $\Sigma_1(e_1,\lambda_1,c_1) = \sigma_1(e_1,\lambda_1,c_1) = 0$ for $e_1 = 0$, and also $\Sigma_2(e_3,\lambda_2,c_2) > 0$ for $e_3 \neq 0$, and $\Sigma_2(e_3,\lambda_2,c_2) = \sigma_2(e_3,\lambda_2,c_2) = 0$ for $e_3 = 0$;
- (P2) $\Sigma_1(e_1,\lambda_1,c_1)$ and $\Sigma_2(e_3,\lambda_2,c_2)$ are twice continuously differentiable with respect to e_1 and e_3 , respectively. Also, the derivative of $\sigma_1(e_1,\lambda_1,c_1)$ is strictly increasing in e_1 for $|e_1| < \rho_1$, and the derivative of $\sigma_2(e_3,\lambda_2,c_2)$ is strictly increasing in e_3 for $|e_3| < \rho_2$, where ρ_1 and ρ_2 are positive constants;
- (P3) there exist four scalar constants $b_{11}, b_{12}, b_{21}, b_{22} > 0$ which satisfy the following constraints

$$b_{11}\sigma_1^2(e_1,\lambda_1,c_1) \le e_1\sigma_1(e_1,\lambda_1,c_1) \le b_{12}\sigma_1^2(e_1,\lambda_1,c_1)$$

$$b_{21}\sigma_2^2(e_3,\lambda_2,c_2) \le e_3\sigma_2(e_3,\lambda_2,c_2) \le b_{22}\sigma_2^2(e_3,\lambda_2,c_2)$$

For the UMS (1), we consider two first-layer switching surfaces as

$$s_1 = e_2 + \sigma_1(e_1, \lambda_1, c_1) \tag{39}$$

$$s_2 = e_4 + \sigma_2(e_3, \lambda_2, c_2)$$
 (40)

For instance, selecting $\sigma_1(e_1,\lambda_1,c_1)=c_1e_1$ and $\sigma_2(e_3,\lambda_2,c_2)=c_2e_3$ gives the two first-layer linear switching surfaces in Equations (30) and (31). The obtained functions, $\Sigma_1(e_1,\lambda_1,c_1)$ and $\sigma_1(e_1,\lambda_1,c_1)$, and also $\Sigma_2(e_3,\lambda_2,c_2)$ and $\sigma_2(e_3,\lambda_2,c_2)$ satisfy the above properties (P1) to (P3).

We construct 2nd-layer switching surface for the system with relative degree two as

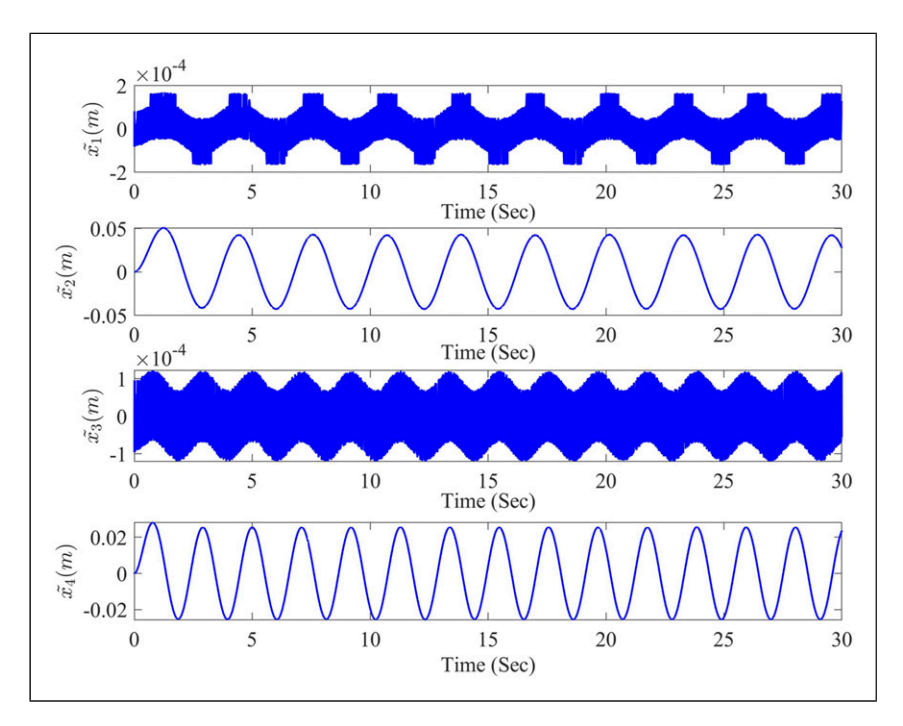


Figure 5. Sliding mode observer estimation errors for angular positions and their velocities.

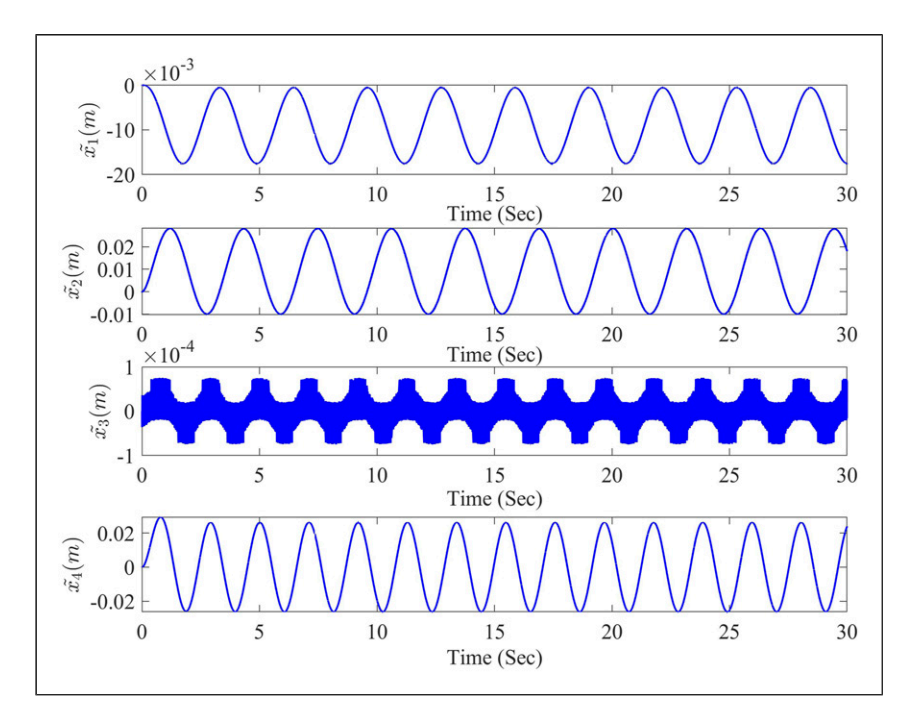


Figure 6. Passivity-based sliding mode observer estimation errors for angular positions and their velocities.

$$S = \alpha s_1 + \beta s_2 = \alpha (e_2 + \sigma_1(e_1, \lambda_1, c_1)) + \beta (e_4 + \sigma_2(e_3, \lambda_2, c_2))$$
(41)

where positive constant control gains α and β are selected such that $\alpha\beta s_1s_2 \ge 0$.

Lemma 6. The UMS (1) with $y = S = \alpha(e_2 + \sigma_1(e_1,\lambda_1,c_1)) + \beta(e_4 + \sigma_2(e_3,\lambda_2,c_2))$ taken as its output is zero-state observable.

Proof. For
$$y = 0$$
, we have $S = \alpha(e_2 + \sigma_1(e_1, \lambda_1, c_1)) + \beta(e_4 + \sigma_2(e_3, \lambda_2, c_2)) = 0$

Now, applying the Lyapunov candidate function as $V(t) = \frac{1}{2}e_1^2 + \frac{1}{2}e_3^2$, its time differential by exerting property (P3) leads to

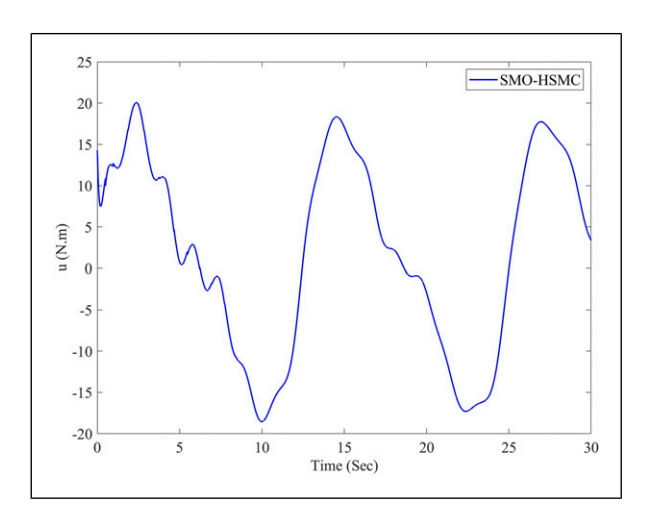


Figure 7. Applied torque u with Sliding mode observer-based hierarchical sliding mode control.

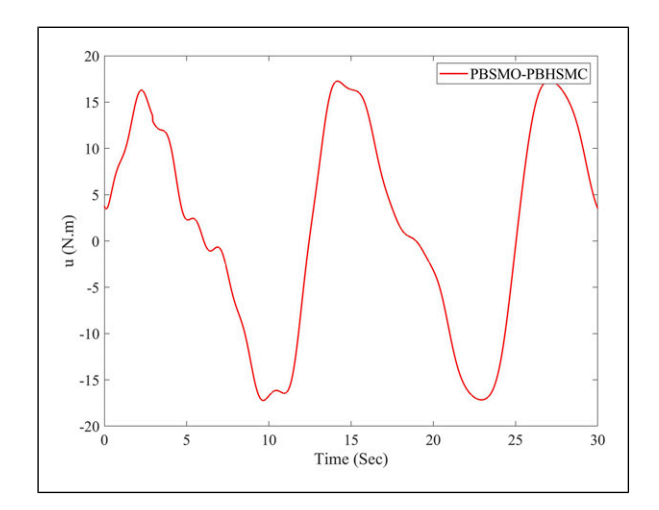


Figure 8. Applied torque *u* with the proposed passivity-based sliding mode observer-based passivity-based hierarchical sliding mode control.

$$\dot{V}(t) = e_1 e_2 + e_3 e_4 = -e_1 \sigma_1(e_1, \lambda_1, c_1) - e_3 \sigma_2(e_3, \lambda_2, c_2)
\leq -b_{11} \sigma_1^2(e_1, \lambda_1, c_1) - b_{21} \sigma_2^2(e_3, \lambda_2, c_2) \leq 0$$

Therefore, $e_i \rightarrow 0$, i = 1, 2, 3, 4 as $t \rightarrow \infty$.

Theory 2. Considering UMS (1) together with the switching surface (41) as a new output of the system, the control law is proposed as

$$u = -\frac{1}{\widehat{g}} \left(\left(\widehat{f}_1 - \dot{x}_{2d} \right) + \frac{e_4}{e_2} \left(\widehat{f}_2 - \dot{x}_{4d} \right) + \sigma_1 + \frac{\sigma_2}{e_2} \left(\widehat{x}_4 - x_{4d} \right) + (k_1 + k_2) \frac{e_2}{|e_2|} + (k_3 + k_4) \frac{s_2}{e_2} \right) + \frac{e_2}{|e_2|^2} Sp$$

$$(42)$$

then UMS (1) has strict passivity with respect to the new output (41). Furthermore, the trajectory errors e converge to zero, that is, $\lim_{t\to\infty} e(t) = 0$. In above equation, p(t) is a continuous time function.

Proof: In order to strictly passivate switching surface (41) using feedback passification, the control law (42) is designable, in which, here, we take S(t) and $z(t) = p(t) - k_3$ as new output and new input, respectively.

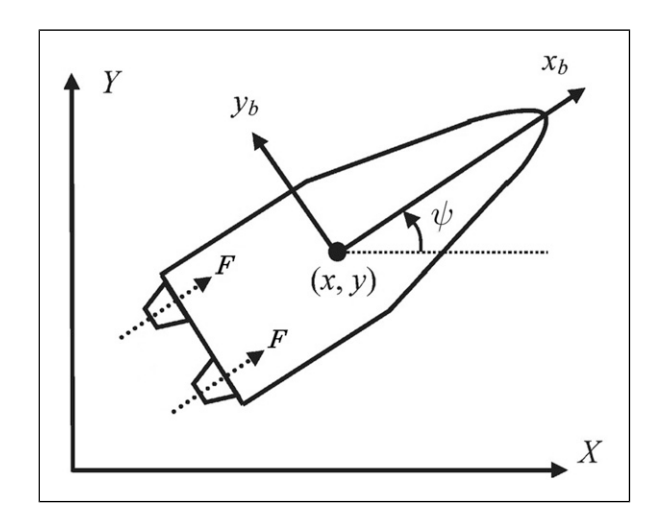


Figure 9. Schematic of planar underactuated surface vessel.

Table 2. Performance comparison of passivity-based hierarchical SM control/passivity-based SM observer with conventional hierarchical sliding mode control/sliding mode observer.

	Passivity-based hierarchical SM control/passivity-based SM observer	hierarchical sliding mode control/sliding mode observer
Tracking	Very good	Good
Chattering	Approximately none	Yes
Presence of unmatched uncertainties	Compensates completely	Cannot reject
Settling time (link position q_l) Overshoot (link position q_l)	Output settles in 2.5 s without overshoot Without overshoot	Output settles in 12 s with overshoot ${\leq}20\%$

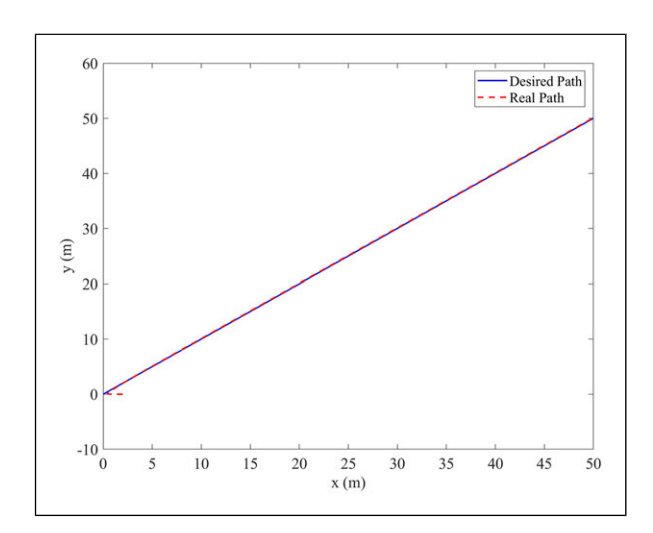


Figure 10. Tracking performance of position.

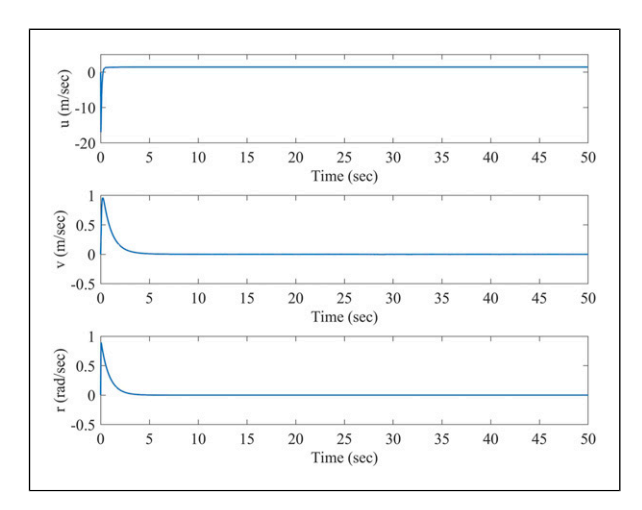


Figure 11. Velocity of surge, sway and yaw.

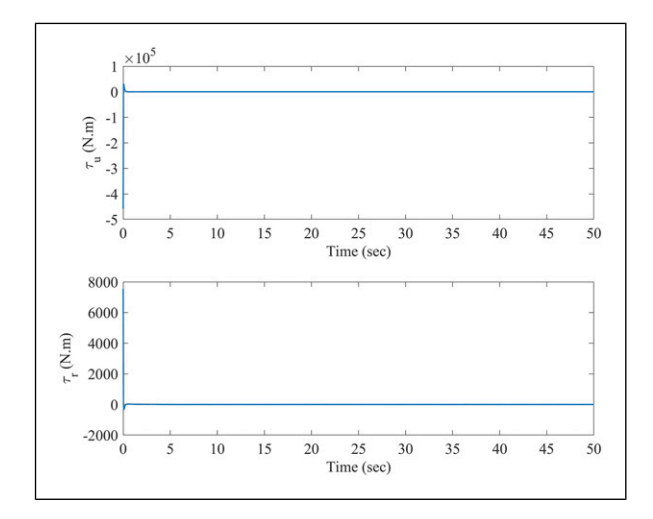


Figure 12. Applied surge force and yaw moment.

By selecting stored energy function like $V(t) = \frac{1}{2}e_4^2 + \frac{1}{2}e_2^2 + \Sigma_2 + \Sigma_1$

$$\begin{split} \dot{V}(t) &= e_4 \dot{e}_4 + e_2 \dot{e}_2 + \frac{\partial \Sigma_2}{\partial e_3} \dot{e}_3 + \frac{\partial \Sigma_1}{\partial e_1} \dot{e}_1 \\ &= e_4 \left(\hat{f}_2 + d_2 - \dot{x}_{4d} + \tilde{f}_2 \right) \\ &+ e_2 \left(\hat{f}_1 + \hat{g}u + d_1 - \dot{x}_{2d} + \tilde{f}_1 + \tilde{g}u \right) \\ &+ \sigma_2 \left(\hat{x}_4 - x_{4d} + \tilde{x}_4 \right) + \sigma_1 \left(\hat{x}_2 - x_{2d} + \tilde{x}_2 \right) \end{split}$$

Substituting control law equation (42) into \dot{V} gives

$$\dot{V}(t) \le -k_1|e_2| - k_3S + Sz = -k_1|e_2| + (p - k_3)S$$

= $-k_1|e_2| + zS$

Integrating the two sides of above equation over $\tau \in [0,t]$ results in

$$\int_{0}^{t} z(\tau)S(\tau)d\tau - k_{1} \int_{0}^{t} |e_{2}(\tau)|d\tau \geq V(t) - V(0)$$

which connotes that the switching surface S(t) with newly defined input z(t) becomes strictly passive. For S(t) = 0, we would conclude from Lemma 6 that $e \to 0$ as $t \to \infty$.

The block diagram presented in Figure 1 resumes the main objective of this work. The control term, z(t), can be obtained by using different techniques. Because the UMS shows strict passivity for control input equation (42), the system provides asymptotic stability even when z=0. If $z=-\varphi(S)$ can be designable such that $\varphi(0)=0$ and $S\varphi(S)>0$ for any $S\neq 0$ and S is considered as an output for the system, UMS (1) with input equation (42) is strictly output passive.

In Theory 2, the control law is developed by employing the passivity property and asymptotic stability can be obtained. The passivation-based HSMC law equation (42) does not provide convergence toward switching surface in finite time. In fact, to satisfy the sliding mode and reaching mode conditions, the control law should be redeveloped and Theory 3 is obtainable.

Theory 3. For UMS (1), the hierarchical switching surface is $S = \alpha(e_2 + \sigma_1) + \beta(e_4 + \sigma_2)$. The designed SMC law as

$$u = -\frac{1}{\widehat{g}} \left(\left(\widehat{f}_1 - \dot{x}_{2d} \right) + \frac{\beta}{\alpha} \left(\widehat{f}_2 - \dot{x}_{4d} \right) + \zeta_1(\mathbf{e}) e_2 \right)$$

$$+\frac{\beta}{\alpha}\zeta_{2}(e)e_{4}+(k_{1}+k_{2})\frac{S}{|S|}$$
 (43)

where $\zeta_1(\mathbf{e}) = \frac{\partial \sigma_1}{\partial e_1}$ and $\zeta_2(\mathbf{e}) = \frac{\partial \sigma_2}{\partial e_3}$, guide the UMS trajectories to reach the switching surface fast and slide on it toward zero tracking error.

Proof: Taking derivative of S(t) yields

$$\dot{S} = \alpha \left(\dot{e}_2 + \frac{\partial \sigma_1}{\partial e_1} e_2 \right) + \beta \left(\dot{e}_4 + \frac{\partial \sigma_2}{\partial e_3} e_4 \right)$$

$$= \alpha \left(\hat{f}_1 + \hat{g}u + d_1 - \dot{x}_{2d} + \tilde{f}_1 + \tilde{g}u + \zeta_1(e) e_2 \right)$$

$$+ \beta \left(\hat{f}_2 + d_2 - \dot{x}_{4d} + \tilde{f}_2 + \zeta_2(e) e_4 \right)$$

By applying $V(t) = \frac{1}{2}S^2$ as Lyapunov function, and substituting the SMC law (43) in \dot{V} guide to

$$\begin{split} \dot{V}(t) &= S\dot{S} \\ &= S\left(\alpha\left(\hat{f}_1 + \hat{g}u + d_1 - \dot{x}_{2d} + \tilde{f}_1 + \tilde{g}u + \zeta_1(e)e_2\right) \\ &+ \beta\left(\hat{f}_2 + d_2 - \dot{x}_{4d} + \tilde{f}_2 + \zeta_2(e)e_4\right) \right) \end{split}$$

Finally, yields in

$$\dot{V}(t) = \alpha S \left(\tilde{f}_1 + \tilde{g}u + d_1 + \frac{\beta}{\alpha} \left(d_2 + \tilde{f}_2 \right) - (k_1 + k_2) \frac{S}{|S|} \right)$$

Applying sufficiently large gains $k_1 + k_2$ leads to $\dot{V}(t) \le -\alpha k_1 \frac{S^2}{|S|}$, where $k_1 > 0$. The inequality ensures that the UMS state trajectories should reach the switching surface in finite time and then slide on the surface.

 Σ_1 and Σ_2 can be considered as energies of subsystems. Since a stable origin exists in a passive system and damping injection is sufficient to stabilize it, whenever e(t) is not identically zero, the energies of subsystems will be dissipated. In the following, we mention some examples and the reader is referred to (Arimoto, 1996; Chang, 2019) for more details.

$$\Sigma_{1}(e_{1},\lambda_{1},c_{1}) = \begin{cases} \frac{1}{2}c_{1}e_{1}^{2}, & |c_{1}e_{1}| < \lambda_{1} \\ \lambda_{1}|e_{1}| - \frac{1}{2c_{1}}\lambda_{1}^{2}, & |c_{1}e_{1}| > \lambda_{1} \end{cases}$$
and
$$\sigma_{1}(e_{1},\lambda_{1},c_{1}) = \begin{cases} \lambda_{1}, & c_{1}e_{1} > \lambda_{1} \\ c_{1}e_{1}, & |c_{1}e_{1}| < \lambda_{1} \\ -\lambda_{1}, & c_{1}e_{1} < -\lambda_{1} \end{cases}$$
(44)

$$\Sigma_{2}(e_{3},\lambda_{2},c_{2}) = \begin{cases} \frac{1}{2}c_{2}e_{3}^{2}, & |c_{2}e_{3}| < \lambda_{2} \\ \lambda_{2}|e_{3}| - \frac{1}{2c_{2}}\lambda_{2}^{2}, & |c_{2}e_{3}| > \lambda_{2} \end{cases}$$
and
$$\sigma_{2}(e_{3},\lambda_{2},c_{2}) = \begin{cases} \lambda_{2}, & c_{2}e_{3} > \lambda_{2} \\ c_{2}e_{3}, & |c_{2}e_{3}| < \lambda_{2} \\ -\lambda_{2}, & c_{2}e_{3} < -\lambda_{2} \end{cases}$$

$$(45)$$

Hence, $\sigma_1(e_1,\lambda_1,c_1) = \lambda_1 sat(c_1e_1,\lambda_1)$ and $\sigma_2(e_3,\lambda_2,c_2) = \lambda_2 sat(c_2e_3,\lambda_2)$. The tangent hyperbolic function is another choice method. It can be resulted that

$$\Sigma_1(e_1, \lambda_1, c_1) = \frac{c_1}{\lambda_1} \ln(\cosh(\lambda_1 e_1)) \quad \text{and}$$

$$\sigma_1(e_1, \lambda_1, c_1) = c_1 \tanh(\lambda_1 e_1) \quad (46)$$

$$\Sigma_2(e_3, \lambda_2, c_2)) = \frac{c_2}{\lambda_2} \ln(\cosh(\lambda_2 e_3)) \quad \text{and}$$

$$\sigma_2(e_3, \lambda_2, c_2) = c_2 \tanh(\lambda_2 e_3) \quad (47)$$

In this method, both design gains c and λ play a role in decision making of the final damping ratio. The control designer has a wide freedom in choosing the potential functions Σ_1 and Σ_2 . It is worthy of mention that Σ_1 and Σ_2 can be different with each other. Different potential functions Σ_1 and Σ_2 can be combined or used together to enhance the system efficiency, for example, equation (44) with equation (47).

5. Simulation Tests

To assess the efficiency of designed controller and observer method, we do their implementation on a single-link flexible-joint manipulator and underactuated surface vessel as our case studies. This section presents results and related discussions of extensive simulation tests carried out by MATLAB/Simulink.

5.1. Flexible-joint manipulator

Figure 2 represents a schematic of single-link flexible-joint manipulator (SFJM) consisting a rigid link of length 2L, mass m, and inertia I, an actuator with inertia of J, and a flexible joint with stiffness K. The length, L stands for the distance between centroid of the flixible link and the joint.

Through the Euler–Lagrange approach (Spong, 1987), the real dynamic model of the SFJM, considering the effects of external disturbances and un-modeled dynamics, can be constructed as (Chang and Yen, 2011; Yan et al., 2021; Zaare and Soltanpour, 2020)

where q_m and q_l stand for the motor angle and link angle, respectively. g denotes the gravitational acceleration and B_m

is the motor damping coefficient; d_m and d_l show unmodeled dynamics and external disturbances related to motor and link variables, respectively. Furthermore, u denotes applied torque by the motor. In such UMS, the elastic torque, $Kq_m - Kq_l$ is the just coupled relation of motor-link dynamics.

$$\begin{cases} J\ddot{q}_{m} + B_{m}\dot{q}_{m} + K(q_{m} - q_{l}) = u + d_{m} \\ I\ddot{q}_{l} + mgL\sin(q_{l}) = K(q_{m} - q_{l}) + d_{l} \end{cases}$$
(48)

For the convenience of representations, new states $x_1 = q_m$, $x_2 = \dot{q}_m$, $x_3 = q_l$, and $x_4 = \dot{q}_l$ are introduced. The motion equation (48) in state-space representation yield

$$\dot{x}_{1} = x_{2}
\dot{x}_{2} = \frac{K}{J}(x_{3} - x_{1}) - \frac{B_{m}}{J}x_{2} + \frac{1}{J}u + d_{1}
\dot{x}_{3} = x_{4}
\dot{x}_{4} = \frac{K}{J}(x_{1} - x_{3}) - \frac{mgL}{J}\sin(x_{3}) + d_{2}$$
(49)

The state-space representation equation (49) is an example for equation (1) with the terms $f_1 = \frac{K}{J}(x_3 - x_1) - \frac{B_m}{J}x_2$, $f_2 = \frac{K}{J}(x_3 - x_1) - \frac{B_m}{J}x_2$ and $g = \frac{1}{J}$. The plant parameter values of the SFJM are listed in Table 1.

Here, the control objective for SFJM is to force actual trajectory of the link to track desired one given by, $x_{3d} = q_{1d} = 0.5 \sin t + \sin(0.5t)$. In following, the trajectory of SFJM link on the desired position together with vibration suppression is the subject of simulations. For the convenience, the initial state vector is assumed to be zero.

The designable parameters for the observer equation (22) and the controller equation (43) can be set as

$$\begin{array}{l} c_1=4.5,\ c_2=5,\ \alpha=7.2,\ \beta=3.8,\ \lambda_1=0.47,\ \lambda_2=0.15,\\ k_1=1.15,\quad \eta_1=0.55,\ \eta_2=0.21,\ \eta_3=0.44,\ \eta_4=0.65,\\ \mu_1=0.2,\ \mu_2=0.88,\ \mu_3=0.12,\ \mu_4=0.28, \\ \eta_1=0.3,\ \overline{w}_2=0.5, \\ r_1(t)=0.1\sin t, \\ r_2(t)=0.05\sin t \end{array}$$

It is worthy to mention that we have employed the same values for the gains common between HSMC/SMO and the proposed approach to assess the both methods under the same conditions. Moreover, we employ saturation function (in both methods) instead of sign function to avoid unwanted chattering phenomena (only in control laws but not in

observer equations) which may be occurred in the control inputs of SMC-based approaches.

To show the significance of our designed method against the recent control methods of SFJM, obtained simulation results are compared with respect to the conventional HSMC-SMO in Figures 3–6.

We can see from Figure 3 that both the designed PBSMO-based PBHSMC and SMO-based HSMC techniques can cause the link follow the desired path. In accordance with Figure 4, tracking error for the angular position of the link reaches to a close region of the origin. According to the tracking error figure, both the techniques can suppress the fast vibrations. In order to assess the tracking effectiveness, both appropriate torque and disturbance suppression ability should be simultaneously considered, because excessively high torques are not applicable in real environment by usual actuators. The simulation results show that the disturbance suppression ability of the PBSMO-based PBHSMC method is better than that of SMO-based HSMC technique (Figure 4). Figures 5 and 6 display estimation errors for the angular positions and their velocities. They show that output estimation errors converge to zero for the both observers in finite time, but the proposed PBSMO has better response with less chattering over the SMO approach. The applied control torques with SMO-based HSMC and the proposed PBSMO-based PBHSMC are depicted in Figures 7 and 8. It can be clearly observed from the torque plots that for a similar output displacement, the SMO-based HSMC technique requires a larger initial peaking torque. With the proposed passivity-based sliding surface both the high overshoot and long settling time issues can be solved simultaneously. Consequently, our proposed approach provides better tracking performance and robustness for the SFJM even despite the presence of input disturbances and unmatched uncertainties. A brief analysis is released in Table 2.

5.2. Underactuated surface vessel

In order to extend the method described for 2-DOFs UMSs, we develop the proposed approach for path tracking of an underactuated surface vessel (USV) as a UMS with 3 DOFs. Figure 9 depicts schematic model for the USV in horizontal plane.

Based on the geometric transformation between motion of the Body $x_b - y_b$ axes and reference X - Y frame of Figure 9 (Fossen, 1994), considering influence of external environmental disturbances and un-modeled dynamics, the actual dynamic model of USV can be established as (Dai et al., 2017, 2018; Huang et al., 2019)

$$\dot{x} = u \cos \psi - v \sin \psi
\dot{y} = u \sin \psi + v \cos \psi
\dot{\psi} = r
\dot{u} = \frac{m_{22}}{m_{11}} vr - \frac{d_{11}}{m_{11}} u + \frac{1}{m_{11}} \tau_u + d_u
\dot{v} = -\frac{m_{11}}{m_{22}} ur - \frac{d_{22}}{m_{22}} v + d_v
\dot{r} = \frac{(m_{11} - m_{22})}{m_{33}} uv - \frac{d_{33}}{m_{33}} r + \frac{1}{m_{33}} \tau_r + d_r$$
(50)

in which x, y, ψ represent longitudinal movement, lateral displacement, and yaw/heading angle, respectively. Also, u, v, r represent surge, sway, and yaw (SSY) velocities, respectively. The parameters m_{11}, m_{22} , and m_{33} denote inherent inertia and added mass coefficients, d_{11}, d_{22} , and d_{33} denote hydrodynamical coefficients of damping. Besides, τ_r and τ_u are the applied control inputs, namely, yaw moment and surge force, respectively. In addition, d_u , d_v , and d_r represent the un-modeled dynamics and the unknown exogenous inputs relating to ocean environment.

We use a global coordinate transformation as (Pettersen et al., 2004)

$$\begin{cases} z_1 = x \cos \psi + y \sin \psi \\ z_2 = -x \sin \psi + y \cos \psi \\ z_3 = \psi \end{cases}$$
 (51)

Then, the resulting model of the vessel become

$$\dot{z}_{1} = u + z_{2}r$$

$$\dot{z}_{2} = v - z_{1}r$$

$$\dot{z}_{3} = r$$

$$\dot{u} = \frac{m_{22}}{m_{11}}vr - \frac{d_{11}}{m_{11}}u + \frac{1}{m_{11}}\tau_{u} + d_{u}$$

$$\dot{v} = -\frac{m_{11}}{m_{22}}ur - \frac{d_{22}}{m_{22}}v + d_{v}$$

$$\dot{r} = \frac{(m_{11} - m_{22})}{m_{33}}uv - \frac{d_{33}}{m_{33}}r + \frac{1}{m_{33}}\tau_{r} + d_{r}$$
(52)

We can define the tracking error system as

$$z_{ie} = z_i - z_{id}, \quad i = 1, 2, 3$$
 (53)

Thereby, the tracking problem of USV is decreased to the stabilization issue of (53). So, we first stabilize 2nd and 3rd subsystems (\dot{v} and \dot{r} equations in equation (52), respectively) with the proposed PBHSMC, and then 1st subsystem (\dot{u} equation in equation (52)) with PBSMC.

Step 1. According to Theory 3, we define total second-layer switching surface as

$$S_{1} = \alpha \left(\dot{z}_{2e} + \sigma_{1}(z_{2e}, c_{1}, \lambda_{1}) \right) + \beta \left(\dot{z}_{3e} + \sigma_{2}(z_{3e}, c_{2}, \lambda_{2}) \right)$$
(54)

The total equivalent control can be obtained as

$$\tau_{r eq} = \frac{m_{33}}{\alpha z_{1} - \beta} \left(\alpha \left[\left(-\frac{m_{11}}{m_{22}} u r - \frac{d_{22}}{m_{22}} v \right) - (u + z_{2} r) r \right] - \ddot{z}_{2d} + \frac{\partial \sigma_{1}}{\partial z_{2e}} \dot{z}_{2e} \right] + \beta \left[\frac{\partial \sigma_{2}}{\partial z_{3e}} \dot{z}_{3e} - \ddot{\psi}_{d} \right] \right) - \left(\frac{(m_{11} - m_{22})}{m_{33}} u v - \frac{d_{33}}{m_{33}} r \right)$$
(55)

The switching control can be designed to be

$$\tau_{r \, sw} = \frac{m_{33}}{\alpha z_1 - \beta} (k_2 S_1 + k_1 \operatorname{sgn}(S_1)) \tag{56}$$

The yaw moment control law is given by

$$\tau_r = \tau_{req} + \tau_{rsw} \tag{57}$$

Step 2. We define the switching surface as

$$S_2 = \dot{z}_{1e} + \sigma_3(z_{1e}, c_3, \lambda_3) \tag{58}$$

Then, we can design the equivalent control by letting $\dot{S}_2 = 0$ as

$$\tau_{u eq} = -m_{11} \left[\frac{m_{22}}{m_{11}} vr - \frac{d_{11}}{m_{11}} u + z_2 \left(\frac{(m_{11} - m_{22})}{m_{33}} uv \right) \right]$$

$$-\frac{d_{33}}{m_{33}} r + \frac{1}{m_{33}} \tau_r + (v - z_1 r) r - \ddot{z}_{1d} + \frac{\partial \sigma_3}{\partial z_{1e}} \dot{z}_{1e}$$
(59)

The switching control part is considered as

$$\tau_{u,sw} = -m_{11}(k_4 S_2 + k_3 \operatorname{sgn}(S_2)) \tag{60}$$

Hence, the surge force control law yields

$$\tau_u = \tau_{ueq} + \tau_{usw} \tag{61}$$

Finally, simulations are carried out on the model of Ref. (Reyhanoglu, 1997). The vessel has the following parameters: $d_{11} = 70$, $d_{22} = 100$, $d_{33} = 50$, $m_{11} = 200$, $m_{22} = 250$, $m_{33} = 80$. Here, desired trajectory to be tracked is considered as a straight line. Hence, for simulation study, it can be figured out that $x_d = y_d = t$ and we assume initial off-tracks for the vessel as, x(0) = 2, $y(0) = \psi(0) = u(0) = v(0) = r(0) = 0$. The parametric uncertainties together with environmental disturbances are assumed to be $d_u = d_v = d_r = 2(-0.5 + rand(.))$, see (Do et al., 2004), in which rand (.) denotes random function with zero

lower bound and a magnitude of 1. The designable parameters for the controller (61) are set as

$$c_1 = 1$$
, $c_2 = 1.25$, $c_3 = 13$, $\lambda_1 = 2$, $\lambda_2 = 1.05$, $\lambda_3 = 1.4$, $\alpha = 0.001$, $\beta = 90$, $k_1 = 0.001$, $k_2 = 100$, $k_3 = 0.001$, $k_4 = 100$

To figure out the superiority of the proposed control method in feasible tracking while dealing with un-modeled dynamics and external disturbances on the USV, numerical simulations are conducted with vivid results in Figures 10–12.

Figure 10 shows the course of the USV trajectory tracking under the proposed control strategy. We can see from Figure 10 that the straight-line tracking performance of the proposed approach is satisfactory. Figure 11 represents the SSY velocities and Figure 12 depicts the applied yaw moment and surge force as well.

6. Conclusions

For underactuated mechanical systems with unmatched disturbance, a combination of passivity-based observercontroller and sliding mode techniques was presented in this paper. First, applying passivation method on observation error dynamics led to design of the state estimator. The newly proposed PBSMO could ensure asymptotic reach of observation errors to the origin. The designed hybrid controller is different from conventional hierarchical sliding mode approach in which it employs feedback passivation to develop the switching surface. A nonlinear two-layer switching manifold was designed based on a stored energy function. It was also taken in the passivation technique as a passive output such that the stability of the whole system was ensured. According to the obtained results, the proposed technique reduces some of control gains while obtains better steady-state and transient performances, in comparison with the conventional HSMC.

Declaration of conflicting interests

The author(s) declared no potential conflicts of interest with respect to the research, authorship, and/or publication of this article.

Funding

The author(s) received no financial support for the research, authorship, and/or publication of this article.

ORCID iD

Mohammad-Reza Moghanni-Bavil-Olyaei https://orcid.org/0000-0002-1432-9611

References

Almeida DIR, Gamez C and Rascón R (2015) Robust regulation and tracking control of a class of uncertain 2DOF

- underactuated mechanical systems. *Mathematical Problems in Engineering* 2015: 1–11.
- Arimoto S (1996) Control Theory of Nonlinear Mechanical Systems. Oxford, UK: Oxford University Press.
- Ashrafiuon H and Erwin RS (2008) Sliding mode control of underactuated multibody systems and its application to shape change control. *International Journal of Control* 81(12): 1849–1858.
- Brockett RW (1983) Asymptotic stability and feedback stabilization. Differential Geometric Control Theory 27(1): 181–191.
- Brogliato B, Lozano R, Maschke B, et al. (2020) *Dissipative Systems Analysis and Control: Theory and Applications*. Berlin, Heidelberg: Springer-Verlag.
- Chalhoub N, Kfoury G and Bazzi B (2006) Design of robust controllers and a nonlinear observer for the control of a singlelink flexible robotic manipulator. *Journal of Sound and Vibration* 291(1–2): 437–461.
- Chang JL (2019) Passivity-based sliding mode controller/observer for second-order nonlinear systems. *International Journal of Robust and Nonlinear Control* 29(6): 1976–1989.
- Chang X-H and Jin X (2022) Observer-based fuzzy feedback control for nonlinear systems subject to transmission signal quantization. Applied Mathematics and Computation 414: 126657.
- Chang Y-C and Yen H-M (2011) Design of a robust position feedback tracking controller for flexible-joint robots. *IET Control Theory & Applications* 5(2): 351–363.
- Chang Y, Zhou P, Niu B, et al. (2021) Switched-observer-based adaptive output-feedback control design with unknown gain for pure-feedback switched nonlinear systems via average dwell time. *International Journal of Systems Science* 2021: 1–15.
- Chawengkrittayanont P and Pukdeboon C (2019) Continuous higher order sliding mode observers for a class of uncertain nonlinear systems. *Transactions of the Institute of Measure*ment and Control 41(3): 717–728.
- Chen L, Wang H, Huang Y, et al. (2020) Robust hierarchical sliding mode control of a two-wheeled self-balancing vehicle using perturbation estimation. *Mechanical Systems and Signal Processing* 139: 106584.
- Choukchou-Braham A, Cherki B, Djemaï M, et al. (2013) Analysis and Control of Underactuated Mechanical Systems. Berlin, Germany: Springer Science & Business Media.
- Dai SL, He S, Wang M, et al. (2018) Adaptive neural control of underactuated surface vessels with prescribed performance guarantees. *IEEE Transactions on Neural Networks and Learning Systems* 30(12): 3686–3698.
- Dai SL, He S and Xu Y (2017) Transverse function approach to practical stabilisation of underactuated surface vessels with modelling uncertainties and unknown disturbances. *IET Control Theory & Applications* 11(15): 2573–2584.
- Do KD, Jiang ZP and Pan J (2004) Robust adaptive path following of underactuated ships. *Automatica* 40(6): 929–944.
- Fantoni I, Lozano R and Sinha S (2002) Non-linear control for underactuated mechanical systems. Applied Mechanics Reviews 55(4): B67–B68.
- Fossen T (1994) Guidance and Control of Ocean Vehicles. New York, NY: John Willey & Sons. Inc.
- Fradkov A (2003) Passification of non-square linear systems and feedback Yakubovich-Kalman-Popov lemma. *European Journal of Control* 9(6): 577–586.

- Hippe P (2006) Windup in Control: Its Effects and Their Prevention. Berlin, Germany: Springer Science & Business Media, 1–20.Undesired Effects of Input Saturation
- Huang H, Gong M, Zhuang Y, et al. (2019) A new guidance law for trajectory tracking of an underactuated unmanned surface vehicle with parameter perturbations. *Ocean Engineering* 175: 217–222.
- Jahangiri F, Talebi HA, Menhaj MB, et al. (2018) A novel scheme for output definition in feedback passivation of nonlinear systems. *International Journal of Systems Science* 49(15): 3196–3201.
- Khalil HK (2002) Nonlinear Systems. Upper Saddle River, NJ: Prentice-Hall.
- Kikuuwe R, Yasukouchi S, Fujimoto H, et al. (2010) Proxy-based sliding mode control: a safer extension of PID position control. *IEEE Transactions on Robotics* 26(4): 670–683.
- Krafes S, Chalh Z and Saka A (2018) A review on the control of second order underactuated mechanical systems. Complexity 2018: 1–17.
- Kurode S, Spurgeon SK, Bandyopadhyay B, et al. (2012) Sliding mode control for slosh-free motion using a nonlinear sliding surface. *IEEE/ASME Transactions on Mechatronics* 18(2): 714–724.
- Liu W, Chen S-Y and Huang H-X (2020) Double closed-loop integral terminal sliding mode for a class of underactuated systems based on sliding mode observer. *International Journal* of Control, Automation and Systems 18(2): 339–350.
- Liu Y and Yu H (2013) A survey of underactuated mechanical systems. IET Control Theory & Applications 7(7): 921–935.
- Moghanni-Bavil-Olyaei M-R, Ghanbari A and Keighobadi J (2019) Trajectory tracking control of a class of underactuated mechanical systems with nontriangular normal form based on block backstepping approach. *Journal of Intelligent & Robotic* Systems 96(2): 209–221.
- Olfati-Saber R (2001) Nonlinear Control of Underactuated Mechanical Systems with Application to Robotics and Aerospace Vehicles. PhD Thesis, Massachusetts Institute of Technology, Cambridge, MA.
- Ortega R, Spong MW, Gomez-Estern F, et al. (2002) Stabilization of a class of underactuated mechanical systems via interconnection and damping assignment. *IEEE Transactions on Automatic Control* 47(8): 1218–1233.
- Pettersen KY, Mazenc F and Nijmeijer H (2004) Global uniform asymptotic stabilization of an underactuated surface vessel: Experimental results. *IEEE Transactions on Control Systems Technology* 12(6): 891–903.
- Qian DW, Liu XJ and Yi JQ (2009) Robust sliding mode control for a class of underactuated systems with mismatched uncertainties. *Proceedings of the Institution of Mechanical Engineers, Part I: Journal of Systems and Control Engineering* 223(6): 785–795.
- Reyhanoglu M (1997) Exponential stabilization of an underactuated autonomous surface vessel. Automatica 33(12): 2249–2254.
- Romero JG, Donaire A, Ortega R, et al. (2018) Global stabilisation of underactuated mechanical systems via PID passivity-based control. *Automatica* 96: 178–185.
- Seron MM, Hill DJ and Fradkov AL (1994) Adaptive passification of nonlinear systems. In: Proceedings of 1994 33rd IEEE Conference on Decision and Control, Lake Buena Vista, FL, 14–16 December 1994, pp. 190–195. IEEE.
- Shi J, Wang J and Fu F (2017) Chatter alleviation for a class of second-order under-actuated mechanical systems with matched

- and mismatched disturbances. *Journal of Vibration and Control* 23(3): 458–468.
- Singh AM and Ha QP (2019) Fast terminal sliding control application for second-order underactuated systems. *International Journal of Control, Automation and Systems* 17(8): 1884–1898.
- Spong MW (1987) Modeling and control of elastic joint robots. *Journal of Dynamic Systems, Measurement and Control* 109(4): 310–318.
- Spong MW (1998) Underactuated mechanical systems. In: Control Problems in Robotics and Automation. Berlin, Germany: Springer, 135–150.
- Tao G and Ioannou PA (1988) Strictly positive real matrices and the Lefschetz-Kalman-Yakubovich lemma. *IEEE Transactions* on Automatic Control 33(12): 1183–1185.
- Tokat S, Fadali MS and Eray O (2015) A classification and overview of sliding mode controller sliding surface design methods. In: Recent Advances in Sliding Modes: From Control to Intelligent Mechatronics. Berlin, Germany: Springer, 417–439.
- Utkin V, Guldner J and Shijun M (1999) Sliding Mode Control in Electro-Mechanical Systems. Boca Raton, FL: CRC Press.
- Wang W, Yi J, Zhao D, et al. (2004) Design of a stable sliding-mode controller for a class of second-order underactuated systems. *IEE Proceedings Control Theory and Applications* 151(6): 683–690.
- Wei X and Mottershead JE (2017) Robust passivity-based continuous sliding-mode control for under-actuated nonlinear wing sections. *Aerospace Science and Technology* 60: 9–19.
- Xu J-X, Guo Z-Q and Lee TH (2013) Design and implementation of integral sliding-mode control on an underactuated two-wheeled mobile robot. *IEEE Transactions on Industrial Electronics* 61(7): 3671–3681.
- Xu R and Özgüner Ü (2008) Sliding mode control of a class of underactuated systems. *Automatica* 44(1): 233–241.
- Xu Z and Rahman MF (2012) Comparison of a sliding observer and a Kalman filter for direct-torque-controlled IPM synchronous motor drives. *IEEE Transactions on Industrial Electronics* 59(11): 4179–4188.
- Yan Z, Lai X, Meng Q, et al. (2021) Tracking control of single-link flexible-joint manipulator with unmodeled dynamics and dead zone. *International Journal of Robust and Nonlinear Control* 31(4): 1270–1287.
- Zaare S and Soltanpour MR (2020) Continuous fuzzy nonsingular terminal sliding mode control of flexible joints robot manipulators based on nonlinear finite time observer in the presence of matched and mismatched uncertainties. *Journal of the Franklin Institute* 357(11): 6539–6570.
- Zehar D, Benmahammed K and Behih K (2018) Control for underactuated systems using sliding mode observer. *International Journal of Control, Automation and Systems* 16(2): 739–748.
- Zhang H, Wang H, Niu B, et al. (2021a) Sliding-mode surfacebased adaptive actor-critic optimal control for switched nonlinear systems with average dwell time. *Information Sciences* 580: 756–774.
- Zhang H, Xu N, Zong G, et al. (2021b) Adaptive fuzzy hierarchical sliding mode control of uncertain under-actuated switched nonlinear systems with actuator faults. *International Journal of Systems Science* 2021: 1–16.